Available online at www.sciencedirect.com
SCIENCE DIRECT
Biochemical Pharmacology 69 (2005) 347–359
Biochemical Pharmacology
www.elsevier.com/locate/biochempharm

Eukaryotic arylamine *N*-acetyltransferase Investigation of substrate specificity by high-throughput screening

Akane Kawamura[a,*], James Graham[a], Adeel Mushtaq[a], Stefanos A. Tsiftsoglou[b], Gregory M. Vath[c], Patrick E. Hanna[c], Carston R. Wagner[c], Edith Sim[a]

[a]*Department of Pharmacology, University of Oxford, Mansfield Road, Oxford OX1 3QT, UK*
[b]*Department of Biochemistry, University of Oxford, South Parks Road, Oxford OX1 3QU, UK*
[c]*Department of Medical Chemistry and Department of Pharmacology, University of Minnesota, Minneapolis, MN 55455, USA*

Received 12 August 2004; accepted 20 September 2004

Abstract

Arylamine *N*-acetyltransferases (NAT; EC 2.3.1.5) catalyse the transfer of acetyl groups from acetylCoA to xenobiotics, including drugs and carcinogens. The enzyme is found extensively in both eukaryotes and prokaryotes, yet the endogenous roles of NATs are still unclear. In order to study the properties of eukaryotic NATs, high-throughput substrate and inhibitor screens have been developed using pure soluble recombinant Syrian hamster NAT2 (shNAT2) protein. The assay can be used with a wide range of compounds and was used to determine substrate specificity of shNAT2. We describe the expression and characterisation of shNAT2 and also purified recombinant human NAT1 and NAT2, including the use of the assay to explore the substrate specificities of each of the enzymes. Hamster NAT2 has similar substrate specificity to human NAT1, acetylating *para*-aminobenzoate but not arylhydrazine and hydralazine compounds. The overlapping but distinct substrate-specific activity profiles of human NAT1 and NAT2 were clearly observed from the screen. Naturally occurring compounds were tested as substrates or inhibitors of shNAT2 and succinylCoA was found to be a potent inhibitor of shNAT2.

Keywords: Arylamine *N*-acetyltransferase; Xenobiotic metabolism; Recombinant protein; High-throughput screening; Arylamines; AcetylCoA/CoA derivatives

1. Introduction

Arylamine *N*-acetyltransferases (NATs: E.C. 2.3.1.5) are a unique family of enzymes that acetylate arylamine, arylhydrazine and arylhydroxylamine compounds using acetyl coenzyme A (acetylCoA) as a cofactor. NATs are found in both eukaryotes [1,2] and prokaryotes [3,4] and are of very similar sizes, ranging from 30 to 34 kDa. More than one NAT isozyme is found in most eukaryotes [2], and in humans, two functional NATs are present, NAT1 and NAT2 [5,6]. The loci encoding the NAT isozymes are highly polymorphic, notably in human *NAT2*, giving rise to fast and slow acetylator phenotypes [7,8]. Epidemiological studies have suggested that various *NAT1* and *NAT2* alleles are linked to increased susceptibility to drug toxicity and cancer risk caused by arylamine exposure [9].

The most common human NAT1*4 and NAT2*4 isoforms share 88% amino acid sequence similarity and 81% identity [5,6]. Despite this level of high homology, human NAT1 and human NAT2 have distinct substrate specificities and tissue distribution [10,11]. Human NAT2 is a xenobiotic-metabolising enzyme that provides a major route to detoxification of drugs such as the anti-tubercular drug isoniazid (INH), the anti-hypertensive drug hydralazine (HDZ) and anti-bacterial sulphonamides. Human NAT2 is mainly expressed in the liver, colon and intestinal epithelium [12–14], which are major sites of drug metabolism.

Abbreviations: NAT, arylamine *N*-acetyltransferase; shNAT2, Syrian hamster NAT2; INH, isoniazid; HDZ, hydralazine; PABA, *para*-aminobenzoate; 4AS, 4-aminosalicylate; 5AS, 5-aminosalicylate; pABGlu, *para*-aminobenzylglutamate; STNAT, *Salmonella typhimurium* NAT; MSNAT, *Mycobacterium smegmatis* NAT; DTNB, 5,5′-dithio-bis(2-nitrobenzoic acid); DLS, dynamic light scattering; IAM, iodoacetamide; CD, circular dichroism; DTT, dithiothreitol

* Corresponding author. Tel.: +44 1865 271595; fax: +44 1865 271853.
E-mail address: akane.kawamura@pharm.ox.ac.uk (A. Kawamura).

0006-2952/$ – see front matter © 2004 Elsevier Inc. All rights reserved.
doi:10.1016/j.bcp.2004.09.014

The known specific substrates of human NAT1 include *para*-aminobenzoate (PABA), 4-aminosalicylate (4AS) and the folate catabolite, *para*-aminobenzylglutamate (pABGlu). In contrast to human NAT2, human NAT1 has a widespread tissue distribution [6,10,14–17], and its expression is detected very early in development [18]. This suggests that human NAT1 has a possible endogenous role in addition to the metabolism of xenobiotics. The endogenous substrate of human NAT1 has been postulated to be pABGlu [19,20], however, this role is yet to be confirmed in vivo. In a recent study, human NAT1 was shown to be overexpressed in breast carcinomas compared to normal breast tissue, and has been proposed to play a role in the development of cancers through enhanced mutagenesis [21]. It has also been suggested that NAT is involved in growth rather than carcinogenesis [22].

Mouse studies have shown that murine NAT2, the human NAT1 homologue, is important in development, where expression is found in adult and embryonic neuronal tissues and also in the embryonic neural tube [23]. It is also found early in development in the heart and gut [23]. Mice lacking either one or both *Nat1* and *Nat2* have no overt phenotype [24,25]; however, further studies are required for detailed analysis of possible compensatory protein expression.

NAT catalyses the acetyl transfer from acetylCoA onto arylamines through an active site Cys residue and a ping-pong mechanism has been identified [26]. The crystal structure of NAT from *Salmonella typhimurium* (STNAT) further revealed that the active site Cys is part of a catalytic triad, Cys–His–Asp, and each of the three residues is conserved throughout the NAT family [27]. This type of catalytic site is reminiscent of cysteine proteases. NATs appear to have different endogenous roles between species. In *Mycobacterium bovis* BCG, NAT is proposed to be involved in cell wall synthesis [28], whereas the NAT homologue in *Amycolatopsis mediterrani*, Rifamycin amide synthase (RifF), has an endogenous role in the rifamycin synthetic pathway [29]. The sequence identity between prokaryotic NAT and eukaryotic NATs is less than 30% and the eukaryotic NAT structure has not yet been solved. Obtaining the structure of eukaryotic NATs is likely to provide insights into their endogenous substrates and functions, as well as their evolutionary divergence.

Two isozymes of NATs have been identified from inbred Syrian (Golden) hamsters [30,31], and the genes have been cloned and sequenced [32–34]. Syrian hamster NAT2 (shNAT2), like human NAT1 and mouse NAT2, acetylates PABA and has a different substrate specificity to Syrian hamster NAT1 [35,36]. Hamster NAT2 is encoded at a polymorphic locus which confers either fast or slow NAT activity [33,35], and has a widespread tissue distribution [37]. As an approach to identifying the endogenous role of human NAT1, we have expressed and purified shNAT2, which can be expressed in *Escherichia coli* [35,38], and has relatively high protein stability [39]. It shares 91% sequence similarity and 81.7% sequence identity with human NAT1 [34]. We have used this recombinant shNAT2 to further characterise the enzyme, and have investigated the effects of alkylating the active site Cys on the stability of the protein. We have performed kinetic screening of shNAT, human NAT1 and NAT2, using an assay method which is suitable for use with a wide range of substrates and inhibitors, including biogenic amines. This allowed, for the first time, an extensive and clear comparison of the different specific activity profiles between the three eukaryotic NATs.

2. Materials and methods

2.1. Materials

The DHFR_shNAT2 fusion protein expression construct pPH70D has been described previously [38]. BL21(DE3)-CodonPlus-RIL competent cells were purchased from Stratagene. All chemicals were purchased from Sigma unless otherwise stated. ÄKTA^{TM} Purifier 10 (P903) and all chromatography equipments, columns (XK16/40) and resins were purchased from APbiotech.

2.2. Expression and purification of recombinant NATs

2.2.1. Hamster NAT2

E. coli cells transformed with pPH70D were grown, and expressed and purified as previously described [38,40] with modifications. TED buffer (20 mM Tris–HCl, pH 7.7, 1 mM EDTA, 1 mM DTT) was used throughout the purification process. The lysate was loaded onto an anion exchange column (DEAE Sepharose) in TED and eluted with a gradient (0.1 M–0.4 M) of NaCl at 1 mL/min. The fractions containing NAT were assayed by detecting the acetylation of PABA using a 96-well plate assay [41]. Fractions containing NAT were eluted at 0.21 M NaCl. The fractions were pooled together and $CaCl_2$ was added to a final concentration of 2.5 mM prior to addition of thrombin (5 U/mg protein). This was incubated for 18 h at 4 °C and dialysed against TED. The dialysed sample was loaded onto the same anion exchange column and the column was eluted with a gradient of NaCl (0.05 M–0.2 M) at 1 mL/min. Fractions were assayed for NAT activity and the active fractions corresponding to 0.1 M NaCl were pooled as above. The sample was concentrated using Centriprep (Millipore) to 1 mL volume and further purified using gel-filtration column chromatography. For alkylation studies, shNAT2 was treated with iodoacetamide as previously described [40].

2.2.2. Gel-filtration chromatography

Gel-filtration experiments were performed using a XK16/40 column packed with Sephacryl S200-HR. For analytical gel filtration, the column was equilibrated with buffer (20 mM Tris–HCl, pH 7.7, 1 mM EDTA, 150 mM

NaCl, 1 mM DTT) and was calibrated [42] using protein standards (porcine thyroglobulin, alcohol dehydrogenase, bovine serum albumin, carbonic anhydrase) at a flow rate of 0.25 mL/min. After concentration, the shNAT2 sample from the second ion exchange column was loaded onto Sephacryl S200HR and eluted at 0.25 mL/min. Absorption was monitored at 280 nm and the fractions were assayed for NAT activity as described above. The purified protein was stored at −80 °C in 5% glycerol.

2.3. Human NAT

2.3.1. Expression and purification of human NAT1*4

Human *NAT1*4*, cloned into pPH70D [43], was transformed into BL21(DE3)CodonPlus-RIL. Human NAT1 was expressed as for shNAT2 modified slightly such that after reaching an absorbance 0.4 at 37 °C, cells were induced with isopropyl-D-thiogalactopyranoside (IPTG) (0.2 mM) for 8 h at 30 °C. Cells containing human NAT1 were lysed and purified using single DEAE anion exchange column, treated with thrombin, dialysed against TED and stored at −80 °C in 5% glycerol.

2.3.2. Expression and purification of human NAT2*4

Human *NAT2*4*, cloned into pET28b(+) [3], was transformed into BL21(DE3)Codon-Plus-RIL and grown in LB, 1 M sorbitol and 2.5 mM betaine at 27 °C. After reaching an absorbance of 0.4, the cells were induced with IPTG (0.75 mM) at 27 °C for 6 h. The purification was performed using Ni^{2+} affinity purification with increasing imidazole concentrations as described in [44] with the addition of 0.2% Triton in the buffers throughout. Purified human NAT2 was dialysed against TED and stored at −80 °C in 5% glycerol.

2.4. Prokaryotic NATs

Recombinant NATs from *S. typhimurium* (STNAT) *and M. smegmatis* (MSNAT) were expressed and purified as previously described [27,44].

2.5. Circular dichroism

Purified protein samples (0.24 mg/mL, 200 μL, in 10 mM sodium phosphate buffer, pH 7.0) were scanned between 200 and 250 nm in a spectropolarimeter in 1 mm cuvette at various temperatures as previously described [45]. For standardisation, spectra were subtracted from the base line spectrum, which was the buffer alone. The temperature equilibrium of the sample was ensured by 5 min incubation prior to each reading.

2.6. Dynamic light scattering

Protein samples (1.5 mg/mL in 20 mM Tris–HCl, pH 7.7, 1 mM EDTA, 1 mM DTT) were subjected to dynamic light scattering (DynaPro Protein Solutions Molecular Sizing Instrument). Scattering by protein solutions was measured 10 times in each preparation.

2.7. Enzyme kinetic assays

N-Acetylation of PABA was measured using 200 μM PABA by the colorimetric detection of remaining arylamine with dimethylaminobenzaldehyde (DMAB) in microtitre plates as previously described [41]. The rate of hydrolysis of acetylCoA by NAT in the presence of a substrate was determined by detecting the free CoA thiol with 5,5′-dithio-bis(2-nitrobenzoic acid) (DTNB) as previously described [46]. The substrate (500 μM) and purified recombinant NAT (routinely 0.25 μg/reaction for shNAT2) in 20 mM Tris–HCl (pH 8.0) buffer were mixed and pre-incubated (37 °C, 5 min) in a 96-well flat-bottom polystyrene plate (Costar®, Corning, Inc.). AcetylCoA was added to a final concentration of 400 μM to start the reaction in a total volume of 100 μL at 37 °C. The reaction was quenched with 25 μL of guanidine hydrochloride solution (6.4 M guanidine–HCl, 0.1 M Tris–HCl, pH 7.3) containing 5 mM DTNB. The absorbance at 405 nm was measured using an Anthos 2020 plate reader. The rate of reaction was such that the hydrolysis of acetylCoA was within the linear range. Controls were carried out in which substrate, acetylCoA or NAT was replaced by the corresponding buffer or solvent solution. The amount of CoA produced in the reaction was determined in comparison with a standard curve. All stock solutions of substrates were dissolved to 100 mM in DMSO and diluted with buffer to give a final concentration of 0.5% DMSO in the reaction mix.

2.8. Modeling of eukaryotic NAT structures

The eukaryotic NAT structures were modeled by spatial restraints using previously determined crystal structures of NAT from STNAT [27] and MSNAT [44] as templates, using the program MODELLER6 [47]. Multiple sequence alignments were made using GCG version 10.0 (Genetics Computer Group, Madison, WI, USA). The final structure integrity was checked using the program PROCHECK [48].

2.9. Antibody generation

Rabbits (New Zealand white strain) were immunised using a 1:1 (v/v) mixture of Freund's Complete Adjuvant (FCA) and purified shNAT2 (0.5 mg, 100 mM NaCl) solution. Four further boosts were performed using a 1:1 (v/v) mixture of Freund's Incomplete Adjuvant (FIA) and purified shNAT2 (0.25 mg, 100 mM NaCl) solution, at 2–4 week intervals. Rabbits were bled 10 days after the final immunisation and the antisera was designated AB199. A pre-immune serum was prepared from the rabbits prior to immunisation.

2.10. Western blot analysis

Protein samples including tissue homogenates (prepared as previously described [18]) were mixed with 14% polyacrylamide SDS-PAGE sample buffer containing 5% (w/v) β-mercaptoethanol and denatured for 10 min at 95 °C. Protein samples were separated using 12% polyacrylamide gels and transferred to a Hybond C nitrocellulose membrane (Amersham) by electrophoresis (25 V, 25 °C for 2 h). The membrane was probed using AB199 at 1:5,000–1:10,000 (v/v) dilution, incubated with mouse anti-rabbit IgG monoclonal antibodies conjugated to horseradish peroxidase at 1:50,000 (v/v) dilution (Sigma) and detected by chemiluminescence (ECL Reagent Kit, Amersham).

3. Results

3.1. Purification of recombinant shNAT2

The purification protocol typically yielded over 30 mg of pure shNAT2 per litre of bacterial culture, allowing simple and fast protein recovery. Analytical gel filtration experiments showed that shNAT2 elutes in a single peak as a monomer (34 kDa) (Fig. 1). A monodispersed peak was observed by dynamic light scattering (DLS), further confirming the homogeneity of the purified protein. Although by mass spectrometry the recombinant protein is 34,230 Da as expected [40] the DLS predicts the protein to have a lower M_w (28 kDa). This result indicates that the shNAT2 is very compactly folded, compatible with the stability of the protein to proteolysis, showing no degradation on storage or with added trypsin up to 10% by weight. However, when the protein is alkylated by iodoacetamide (IAM), shNAT2 becomes more susceptible to proteolysis on storage (Fig. 2b). N-terminal sequencing of fragments, designated 2–4 in Fig. 2b, of both shNAT2 and IAM_shNAT2 revealed that the protein was cleaved from the C-terminus.

With extended shNAT2 storage time (60 days, Fig. 2), shNAT2 peaks of higher molecular weights are observed on gel filtration, indicating aggregation or oligomerisation. All fractions from higher molecular weight peaks ran as monomeric 34 kDa bands after reduction with β-mercaptoethanol (Fig. 2a), however these peaks did not have any catalytic activity. This is very similar to what has been observed with recombinant MSNAT [44].

3.2. Thermal stability of shNAT2

Hamster NAT2 was incubated at temperatures from 4 to 70 °C. The NAT activity dramatically drops after incubation above 45 °C (Fig. 3a). This corresponds to the thermal denaturation patterns observed in circular dichroism (CD) spectra of shNAT2, where the protein starts to lose its structural fold at a temperature between 45 and 50 °C temperature (Fig. 3b). The thermal stability profile of shNAT2 follows a similar pattern to that of human NAT1 [49], as well as the prokaryotic enzymes STNAT [50] and MSNAT [44]. In order to investigate whether shNAT2 could refold following thermal denaturation at 90 °C, the heat-treated shNAT2 enzyme solution was

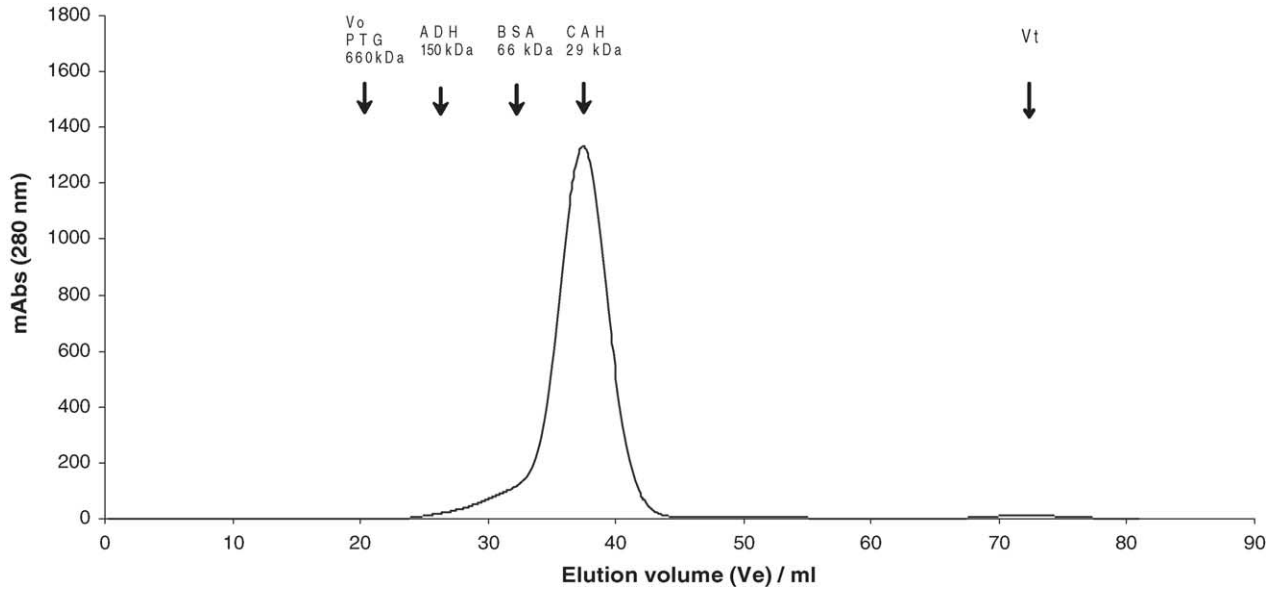

Fig. 1. Analytical gel filtration: Sephacryl S-200 HR elution profile of shNAT2. Fractions containing shNAT2 from the 2nd DEAE column (Table 1) were concentrated to 1 mL and loaded onto a Sephacryl S-200 HR column (XK16-40). The protein was eluted in TED buffer (20 mM Tris–HCl, pH 7.7, 1 mM EDTA, 100 mM NaCl, 1 mM DTT) at a flow rate of 0.25 mL/min at 4 °C. Hamster NAT2 was eluted at 37.6 mL, calculated as 34 kDa against the protein standards. Protein standards: PTG: porcine thyroglobulin (M_w 660,000, V_e = 21.26 mL), ADH: alcohol dehydrogenase (M_w 150,000, V_e = 27.08 mL), BSA: bovine serum albumin (M_w 66,000, V_e = 33.31 mL), CAH: carbonic anhydrase (M_w 29,000, V_e = 38.64 mL), V_o: void volume (21 mL), V_t: packed bed total volume (74 mL).

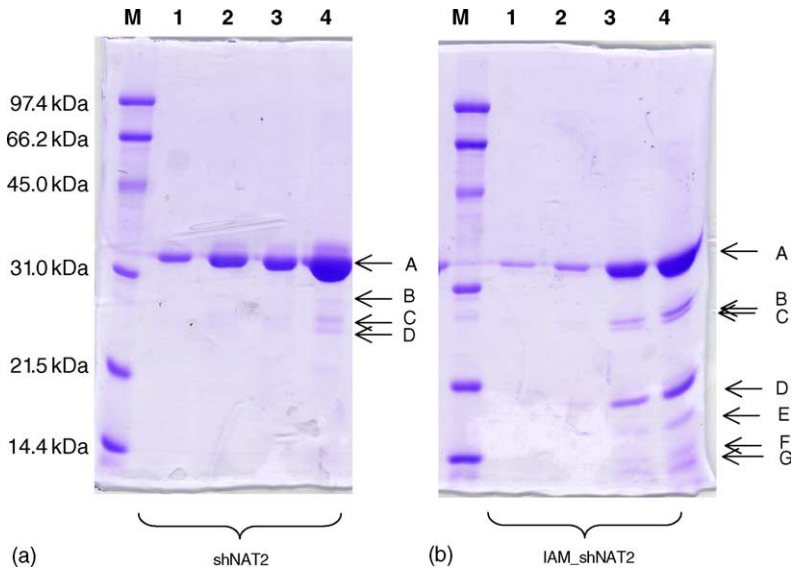

Fig. 2. Comparison of the stability of hamster NAT2 with and without alkylation. Monomeric gel-filtered shNAT2 and IAM_shNAT2 were stored at 20 mg/mL in 20 mM Tris–HCl, 1 mM EDTA, 1 mM DTT buffer with 5% glycerol at −20 °C for 60 days. Various concentrations of the protein were loaded onto a 14% SDS-PAGE and stained with Coomassie blue. The protein band fragment molecular weights were calculated against protein standards using a log plot. Lanes: Gel (a) 1 = 2 μg, 2 = 4 μg, 3 = 20 μg, 4 = 40 μg, A = 33 kDa, B = 25.8 kDa, C = 22.7 kDa, D = 21.2 kDa; Gel (b) 1 = 4 μg, 2 = 8 μg, 3 = 40 μg, 4 = 80 μg, A = 33 kDa, B = 24.5 kDa, C = 23.4 kDa, D = 15.9 kDa, E = 14.9 kDa, F = 12.7 kDa, G = 10.8 kDa. Lane M indicates molecular weight markers (left-hand side) on both gels (a) and (b).

cooled to room temperature and re-scanned using CD, however no re-folding was observed after 18 h, nor was activity restored.

3.3. Polyclonal antibody is eukaryotic NAT-specific

Polyclonal antibody 199 (AB199) was generated against purified hamster NAT2. The resulting antibody, AB199, was NAT-specific, with clean and successful detection of recombinant hamster NAT2 (Fig. 4a) and NATs from hamster liver at a high antiserum titre (1:10,000, v/v) (Fig. 4b). AB184, a human NAT1-specific antibody [51], also cross-reacts with hamster NAT2. The AB199 cross-reacts with other eukaryotic NATs, including recombinant human NAT1 and NAT2 (Fig. 4c). Due to the recombinant human NATs being partially purified, the relative intensity of the Western blot does not reflect the relative affinity for the different NATs. The antibody was

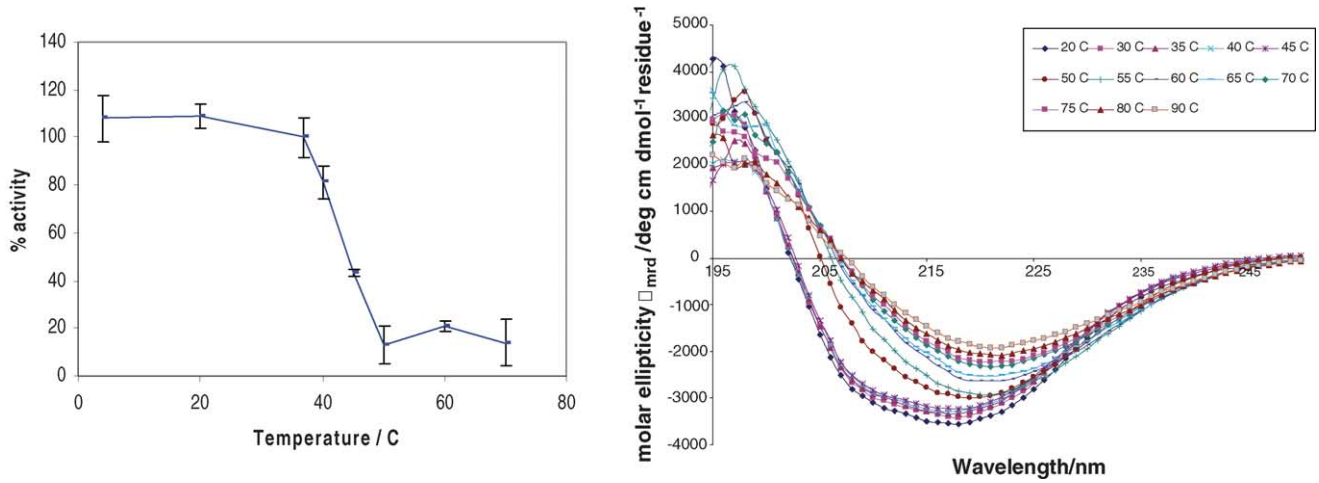

Fig. 3. Effect of temperature on shNAT2. (a) The specific activities of shNAT2 following incubation at different temperatures were determined using acetylation of PABA. The reaction mix (50 ng shNAT2, 200 μM PABA, 1 mM DTT in 20 mM Tris–HCl, pH 8.0) was pre-incubated at various temperatures (as indicated) before the specific rate was assayed at 37 °C. (b) Circular dichroism was used to monitor thermal denaturation of shNAT2 as described in Section 2. The mean molar ellipticity per residue (θ_{mrd}) was measured after incubation at various temperatures as indicated, between the wavelengths 195–250 nm and is shown as individual spectra (b).

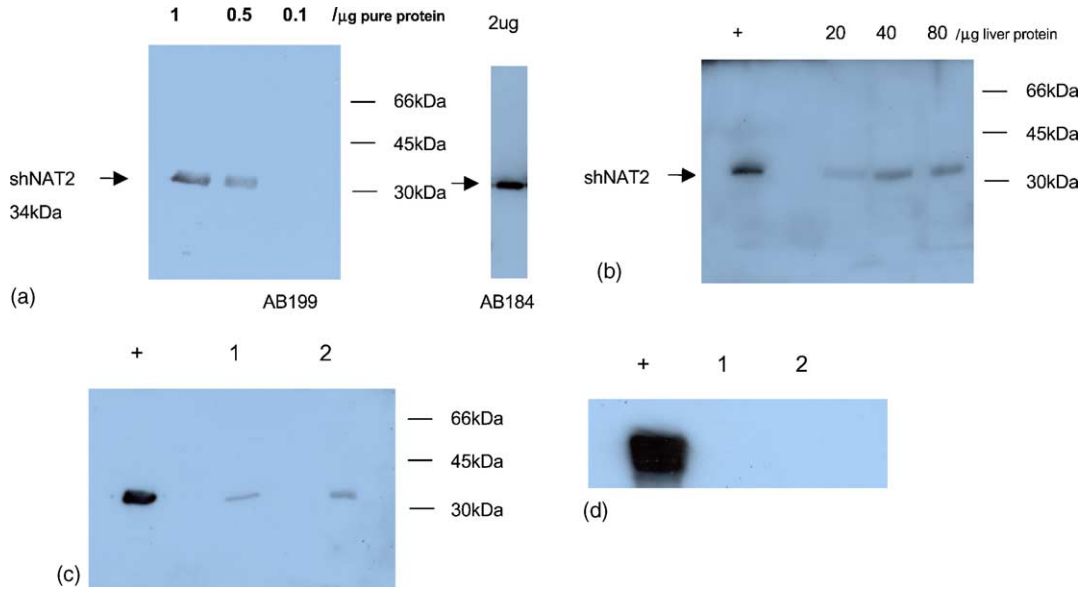

Fig. 4. Specificity of an antibody raised against whole shNAT2 using Western blotting. (a) Purified recombinant shNAT2 (1, 0.5, 0.1 μg) was probed using AB199 (1:10,000, v/v). A single band of 34 kDa was detected. AB184 [51] (1:2000, v/v) was used as a control. Western blotting was used to detect NATs from (b) Syrian hamster liver homogenate (20, 40, 80 μg protein), (c) recombinant human NAT1 and NAT2, and (d) pure recombinant prokaryotic NATs from *S. typhimurium* and *M. smegmatis* (5 μg each) using (1:5,000, v/v) of the AB199. Pure recombinant shNAT2 (0.5 μg) was used as a control (b–d).

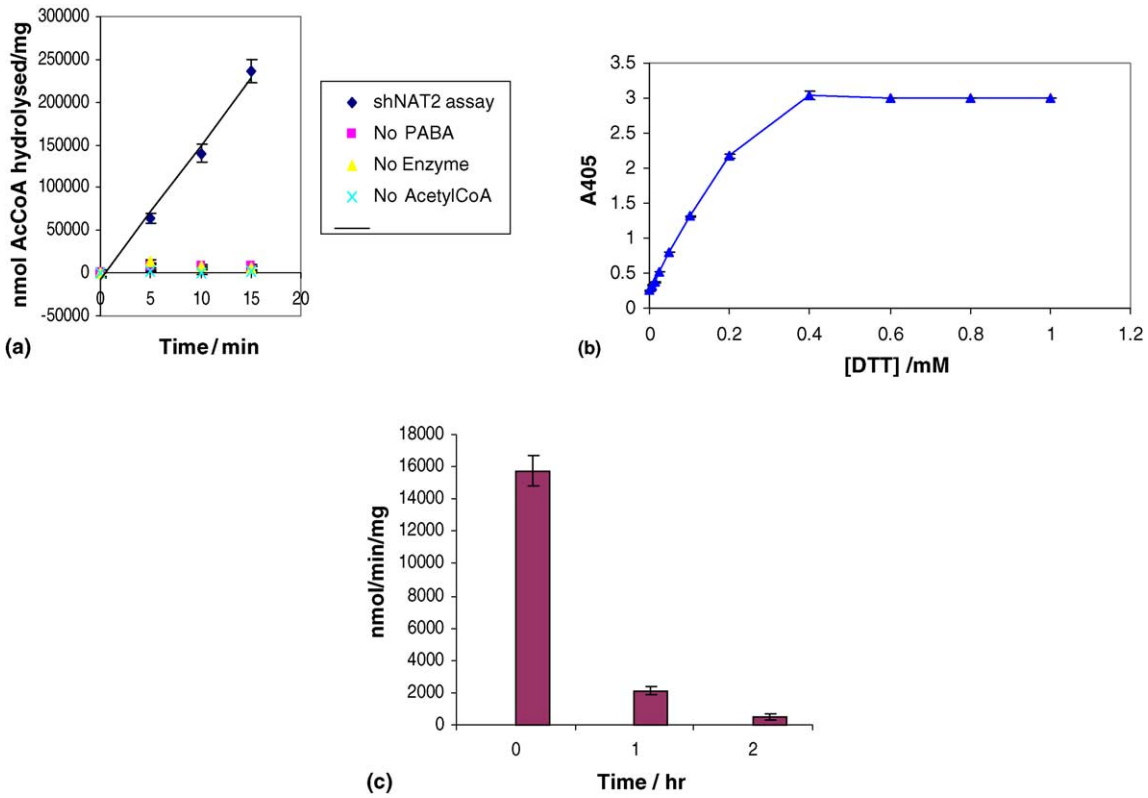

Fig. 5. Measurement of shNAT2 activity by hydrolysis of acetylCoA. (a) The time course for acetylCoA hydrolysis with shNAT2 and PABA (500 μM) is shown. In the control reaction (◆), shNAT2 (0.25 μg) was incubated at 37 °C with PABA (500 μM) for 5 min prior to the addition of AcCoA (400 μM). The reaction was stopped after 5, 10 or 15 min and the DTNB was added to develop colour. Reactions were performed using the same method but replacing PABA (⊞), shNAT2 (▲), AcetylCoA (×) with the corresponding solution. (b) Varying concentrations of DTT (100 μL) was reacted with DTNB (25 μL) and the absorbance was measured at 405 nm. (c) Purified recombinant shNAT2 (0.5 mg/mL) in TED buffer (20 mM Tris–HCl, pH 7.7, 1 mM EDTA, 1 mM DTT) with 5% glycerol, was diluted 20-fold in assay buffer at 4 °C. The diluted protein sample was incubated either immediately with PABA or incubated for 1 or 2 h at 37 °C before assaying the activity with PABA (500 μM). The reaction mix was incubated for further 5 min at 37 °C before addition of acetylCoA (400 μM). The reaction was stopped after 10 min incubation by addition of guanidine HCl.

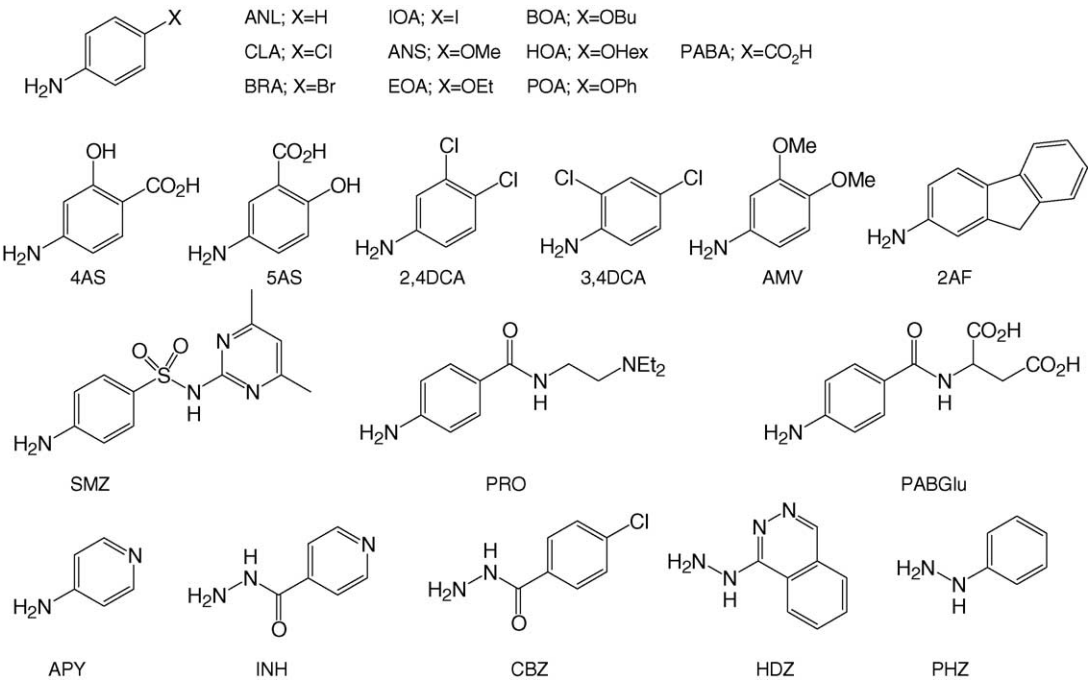

Fig. 6. Chemical structures of arylamine and arylhydrazine compounds tested as substrates. Abbreviations used for compounds are as follows: aniline (ANL), 4-chloroaniline (CLA), 4-bromoaniline (BRA), 4-iodoaniline (IOA), 4-anisidine (ANS), 4-ethoxyaniline (EOA), 4-butoxyaniline (BOA), 4-hexyloxyaniline (HOA), phenoxyaniline (POA), 4-aminobenzoate (PABA), 5-aminosalicylate (5AS), 4-aminosalicylate (4AS), 2,4-dichloroaniline (2,4DCA), 3,4-dichloroaniline (3,4DCA), 4-aminoveratrole (AMV), 2-aminofluorene (2AF), sulphamethazine (SMZ), procainamide (PRO), *para*-aminobenzoyl-L-glutamate (PABGlu), aminopyridine (APY), isoniazid (INH), 4-chlorobenozoic hydrazide (CBZ), hydralazine (HDZ) and phenylhydrazine (PHZ).

tested on pure recombinant prokaryotic NATs, including STNAT and MSNAT but no cross-reactivity was observed with these enzymes (Fig. 4d).

3.4. Kinetic studies of eukaryotic NATs

In order to screen a broad range of NAT substrates under the same conditions and methodology, we have adapted an assay which has been previously employed for the characterisation of prokaryotic NATs [46]. The assay is based on the observation that hydrolysis of acetylCoA occurs only in the presence of a substrate. A series of compounds were screened as substrates by assaying the rate of hydrolysis of acetylCoA. Initially, the assay conditions were optimised using purified shNAT2. Using this assay, we detected no spontaneous hydrolysis of acetylCoA in the absence of substrate and the activity was linear during the assay time interval with purified shNAT2 (Fig. 5a). The limitation of this method is that the assay is sensitive to thiol-containing reagents, since DTNB reacts with free thiols. The assay was performed with the concentration of dithiothreitol (DTT) below 10 μM (Fig. 5b) so that hydrolysis of acetylCoA in the presence of NAT could be detected. Hamster NAT2 contains five Cys residues, and the active site Cys is highly sensitive to oxidation [52]. It was initially necessary to determine conditions under which shNAT2 would be active in the presence of 10 μM DTT. Hamster NAT lost activity at 10 μM DTT (Fig. 5c), but could be assayed reproducibly by storing samples in 1 mM DTT and diluting immediately prior to determination of activity.

3.5. Hamster NAT2-specific activity profile

With a range of arylamine and arylhydrazine compounds (Fig. 6), it was demonstrated that 2-aminofluorene (2AF) and *para*-aminobenzic acid (PABA) are substrates of shNAT2, consistent with previous findings [31,35] (Fig. 7a). 4AS was also confirmed to be a substrate which was acetylated more rapidly than 5AS.

In contrast, shNAT2 does not acetylate isoniazid (INH), hydralazine (HDZ) nor any of the other arylhydrazine compounds tested. The rate of acetylation of haloanilines (4-iodoaniline (IOA) > 4-bromoaniline (BRA) > 4-chloroaniline (CLA)) by shNAT2 is reduced with increasing electronegativity of the halogen substituent. The rate of acetylation of alkoxyanilines (4-anisidine (ANS) > 4-ethoxyaniline (EOA) > 4-butoxyaniline (BOA) > 4-hexoxyaniline (HOA)) by shNAT2 decreases with increasing steric bulk of the alkoxy substituent. Hamster NAT2 does not acetylate sulfamethazine (SMZ) and procainamide (PRO).

3.6. Human NAT-specific activity profile

Following optimisation of the assay using shNAT2, partially purified recombinant human NAT1 and NAT2

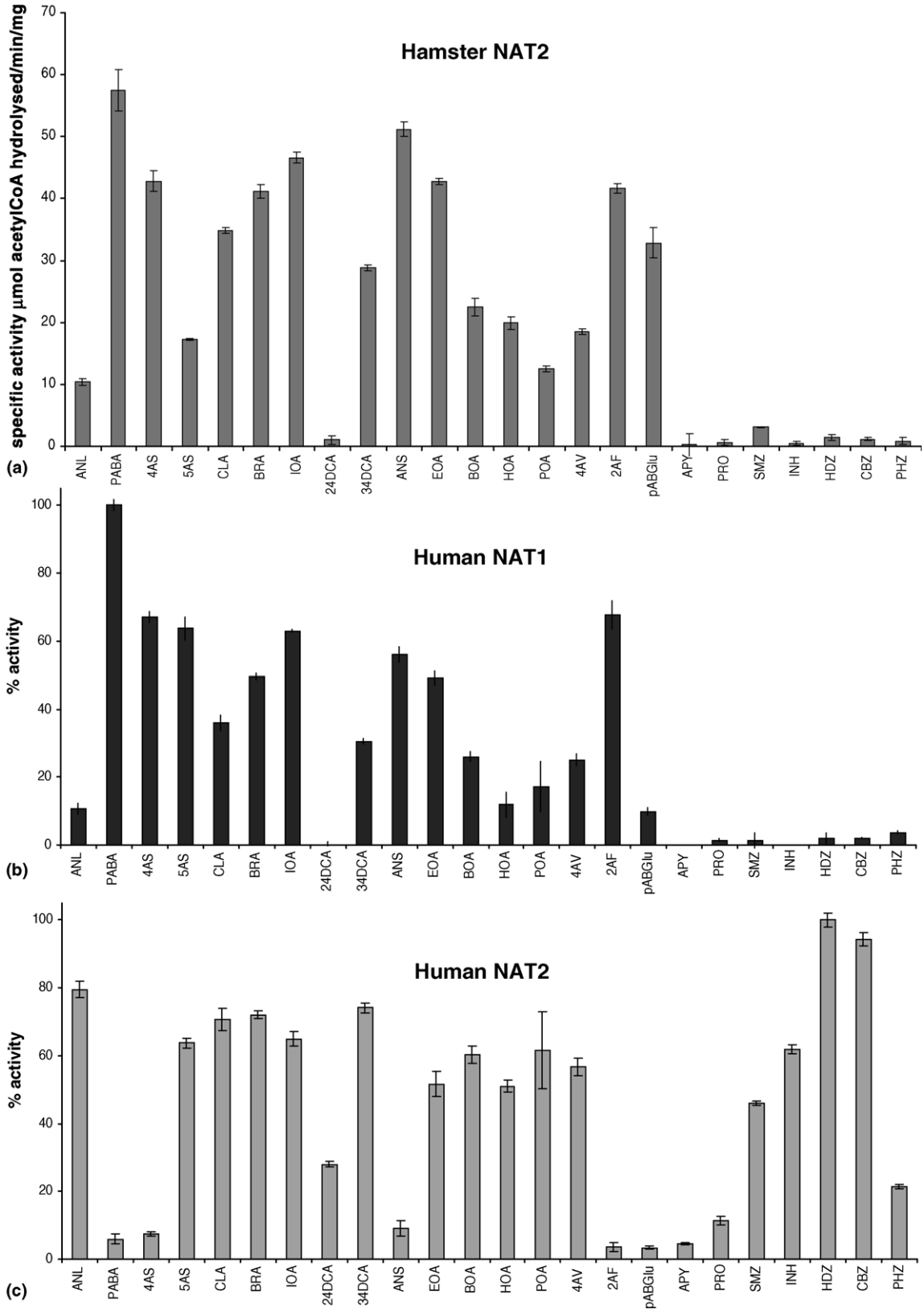

Fig. 7. Screening of potential substrates of NAT and isozymes by measuring hydrolysis of acetylCoA. The activity of shNAT2 was determined by measuring the rate of hydrolysis as described in the methods. Purified shNAT2 (0.25 μg) (a) and partially purified human NAT1 (b) and human NAT2 (c) were each tested against a wide range of substrates (each at 500 μM) and incubated with 400 μM acetylCoA in assay buffer (20 mM Tris–HCl, pH 8.0) in 0.5% DMSO at 37 °C. The specific activity was determined over the linear range. All measurements were performed three times and are described as average ± standard deviation.

were used to screen for substrates using the same high-throughput method and under the same substrate concentrations. There was no spontaneous hydrolysis observed in the absence of substrates for either human NAT isozyme. All the activities are described in percentage activity relative to the best substrate (Fig. 7b and c), in order to allow direct comparison of the partially purified isozymes.

Consistent with previous findings [31], human NAT1 shows the maximum acetylation activities with PABA and 4AS, whereas none of the arylhydrazine compounds tested were substrates (Fig. 7b). Human NAT1 also acetylates 5AS. The specific activity of alkoxyanilines decreased as chain length increases (ANS > EOA > BOA > HOA). The rate of acetylation of haloanilines by human NAT1 decreases with increasing electronegativity of the halogen atom.

In contrast, arylhydrazine compounds were amongst the best substrates for human NAT2 (Fig. 7c). However, a carboxylic group in the *para*-position greatly decreases the rate of acetylation by human NAT2 such that 4AS and PABA are not substrates. Nevertheless, 5AS with a carboxylic group in the *meta*-position is a substrate for both human NAT1 and NAT2.

3.7. Hamster NAT2 natural substrate/inhibitor screening

With the aim of identifying a possible endogenous role of NAT, we tested a range of natural compounds as substrates or inhibitors using shNAT2 under the same conditions as the exogenous compound screen. None of the biogenic amine compounds were effective substrates or inhibitors of shNAT2 (Fig. 8, Table 1).

A series of acetylCoA derivatives were tested as cofactors of shNAT2 (Fig. 8). The hydrolysis of the thiol ester was measurable with butyrylCoA and propionylCoA but at a slower rate than with acetylCoA. The activity decreased with increasing acyl chain length, and very little hydrolysis was observed above an acyl chain length 6. Interestingly, when CoA derivatives were tested as inhibitors of shNAT2, there was a pronounced inhibition of shNAT2 activity by succinylCoA with an IC_{50} of approximately 3 μM. However, other carboxylate CoA derivatives did not act as potent inhibitors (Table 1).

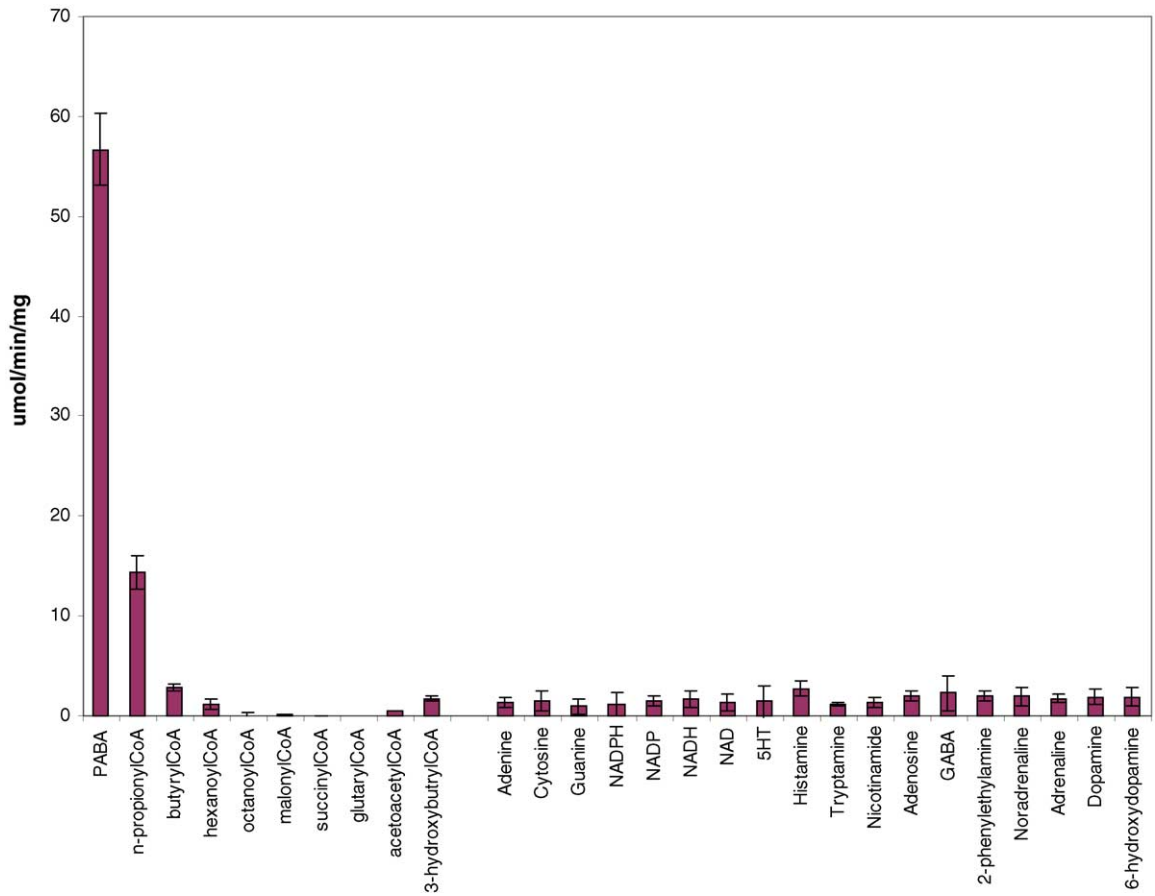

Fig. 8. Screening for endogenous substrates of shNAT2. The biogenic amines (each at 500 μM) were tested as substrates of shNAT2 under the same conditions as described in Fig. 7. CoA derivatives (400 μM) were tested as substrates of shNAT2 using PABA (500 μM) as the arylamine substrate. All reactions were performed in triplicates and results are shown as the average activity ± standard deviation.

Table 1
Screening of potential inhibitors of shNAT2

100 μM	% Activity
Biogenic amines	
Control PABA/AcCoA	100 ± 4
Adenine	98 ± 6
Cytosine	97 ± 6
Guanine	92 ± 7
NADPH	97 ± 4
NADP	100 ± 4
NADH	96 ± 4
NAD	87 ± 8
5HT	95 ± 5
Histamine	100 ± 6
Tryptamine	99 ± 6
Nicotinamide	93 ± 2
Adenosine	95 ± 2
GABA	95 ± 7
2-Phenylethylamine	97 ± 7
Noradrenaline	87 ± 7
Adrenaline	89 ± 2
Dopamine	92 ± 9
CoA derivatives	
n-PropionylCoa (*n* = 1)	94 ± 5
ButyrylCoa (*n* = 2)	72 ± 6
HexanoylCoa (*n* = 4)	76 ± 2
OctanoylCoA (*n* = 6)	26 ± 2
MalonylCoA (*n* = 1)	89 ± 3
SuccinylCoA (*n* = 2)	4 ± 3
GlutarylCoA (*n* = 3)	66 ± 4
AcetoacetylCoA	56 ± 24
3-HydroxybutrylCoA	100 ± 13

Biogenic amines (100 μM_{final}) were incubated with shNAT2 (0.25 μg) and PABA (500 μM_{final}) for 5 min at 37 °C prior to addition of AcetylCoA (400 μM_{final}) to start the reaction. For CoA derivatives, the CoA derivatives (100 μM_{final}) were incubated with shNAT2 (0.25 μg) and ActylCoA (400 μM_{final}) prior to the addition of PABA (500 μM_{final}) to start the reaction. The percentage activity was determined relative to the reaction with PABA and acetylCoA only. All reactions were performed in triplicates and results are shown as the average activity ± standard deviation.

4. Discussion

shNAT2 has been purified to homogeneity in high yield. The large molecular weight aggregation peaks identified in previous studies [38] only appear on storage of the pure protein. These aggregates are inactive but migrate as single 34 kDa band on SDS-PAGE with reduction prior to electrophoresis. Following purification, the protein is a highly stable compacted monomer. Hamster NAT2 is particularly stable to proteolysis on storage. However, if the protein is alkylated with iodoacetamide, the protein is degraded more readily. The proteolytic digestions observed for alkylated protein after long-term storage is unlikely to be due to denaturation of shNAT2, as the CD profile of the alkylated protein closely resembles that of the native shNAT2, but could be due to a conformational change with alkylated protein which is not detectable by CD.

The purified shNAT2 has enabled high-throughput screening of a wide range of substrates. Using the screening methods optimised for shNAT2, human NAT1 and NAT2 were also screened in a similar fashion. The screen confirmed that human NAT1 and NAT2 have overlapping but very distinct specific activity profiles, and that the shNAT2 closely resembles the profile of human NAT1 rather than human NAT2.

The substrate screen demonstrated that none of the arylhydrazine compounds are substrates of human NAT1. Human NAT2, on the other hand, can acetylate arylhydrazine compounds. For haloanilines, there is an increase in activity of human NAT1 with decreased inductive effect, and this is also consistent with the reduced activity of the 2,4-dichloroaniline (2,4DCA) compared to 3,4-dichloraniline (3,4DCA). The lack of specific activity detected for 2,4DCA could also be a result of the steric hindrance of the chlorine substitution in the *ortho*-position. In contrast, human NAT2 does not appear to be sensitive to the differing inductive effects of the halogen atoms, with the activity for all mono-halogenated compounds being similar.

In the alkoxyaniline series, the alkoxy group becomes more electron-donating with chain length, making the amine more nucleophilic, however this is in competition with the increase in the steric bulk, which is likely to be the dominant factor. In human NAT1, the decrease in activity with increased alkoxy chain length may be due to the small size of the active site pocket of human NAT1. In contrast, human NAT2 has very similar activity towards different alkoxyanilines, including phenoxyaniline (POA) and 4-aminoveratrole (4AV), suggesting that human NAT2 is less sensitive to the steric bulk of the substrate than human NAT1.

Anilines containing a *para*-carboxylic acid substituents (4AS and PABA) are good substrates of human NAT1 but not human NAT2. Site-directed mutagenesis studies have shown both Phe^{125} and Arg^{127} are crucial for human NAT1 to acetylate 4AS. In human NAT2, Ser is present instead of Phe^{125} and Arg^{127}. Substitution of either or both Ser^{125} and Ser^{127} in human NAT2 decreases the affinity towards 4AS [53]. A computational model of human NAT1 shows that Phe^{125} is positioned 6 Å away from Cys^{68} (Fig. 9), and aligned with Arg^{127}, a residue where substrate interaction is likely to occur. In both shNAT2 and human NAT1, it is possible that Arg^{127} is hydrogen bonding to the *para*-carboxylic acid groups of PABA and 4AS, and Phe^{125} is involved in aligning the substrate, making them favourable shNAT2 and human NAT1 substrates. 5AS is acetylated readily by both human NAT1 and NAT2 and this may well be important in metabolism of this drug which is used for inflammatory bowel disease, since both human NAT1 and NAT2 are expressed in the intestine [14].

A 3D crystal structure of a eukaryotic NAT is required with and without substrate bound before the model can be fully assessed. In order to test whether these interactions between enzymes and substrate take place, a 3D structure of a eukaryotic NAT is required at high resolution. Diffractable crystals of shNAT2 have not been obtained despite numerous attempts. The lack of diffractable crystals may be due to the presence of an interdomain loop [3], which is found in all the eukaryotic NATs.

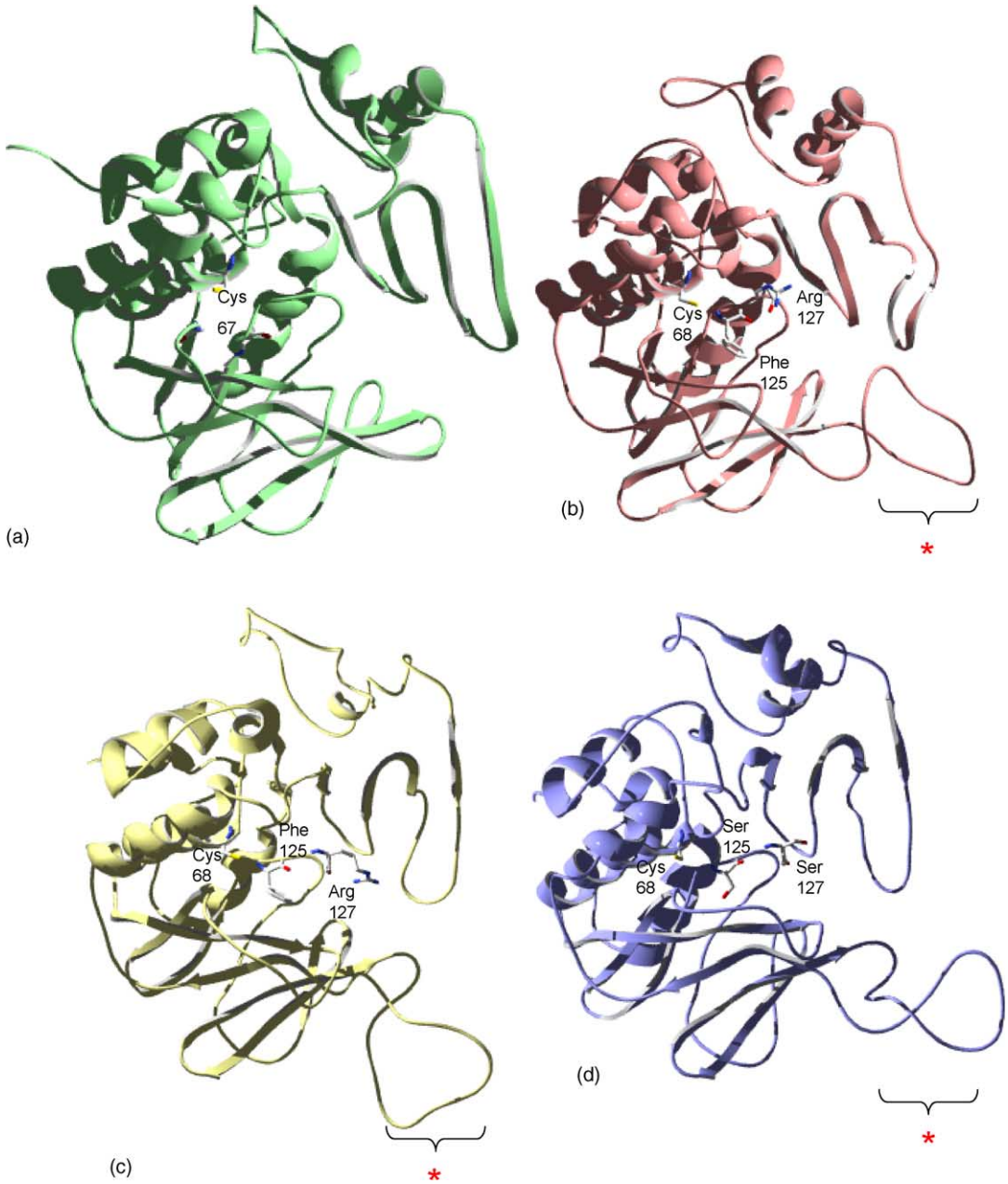

Fig. 9. MSNAT crystal structure and eukaryotic NAT models. (a) A crystal structure of the MSNAT monomeric unit at 1.7 Å (PDB Code 1GX3). Eukaryotic NATs ((b) hamster NAT2, (c) human NAT1, (d) human NAT2) were constructed using MODELLER. The putative inter-domain loop region is shown (*) for eukaryotic NAT models.

It has been previously discussed that pABGlu, a folate catabolite, is a specific substrate for human NAT1 [19,20]. We have observed, under the conditions used here, that pABGlu is a better substrate for hamster NAT2 than for human NAT1, which in turn metabolises pABGlu better than other human isoenzyme NAT2. The results obtained with human NAT1 further confirm the functional similarity between human NAT1 and hamster NAT2. However, the observations that succinylCoA, and to a lesser extent acetoacetylCoA, act as inhibitors, may indicate that NAT has a role related to acetylCoA metabolism, as has been suggested by patterns of NAT expression in cells [54,55]. Recent studies on expression during embryonic development suggest that the expression pattern in the heart alters when metabolism is transferred from glucogenic to ketogenic [56]. In mycobacteria, NAT appears to be involved in specific lipid synthesis [28]. These studies need to be extended to eukaryotic cells where control of NAT expression is beginning to be understood.

5. Conclusion

Purified recombinant shNAT2 was used to screen for substrates and inhibitors using high-throughput methods in order to define an extensive specific activity profile of

shNAT2, with which to compare with the profiles of human NAT1 and NAT2. Our results indicate the clear distinction between the human NAT1 and NAT2 activities, and the similarity between shNAT2 and human NAT1. Screening of endogenous substrates has identified succinylCoA to have a very potent inhibitory effect on shNAT2. The physiological significance of this requires further investigation. In addition, the assay method described provides the basis for high-throughput screening of compounds as potential ligands of eukaryotic NATs as has been demonstrated previously with the prokaryotic NAT enzymes [46].

Acknowledgements

We thank Haiqing Wang (University of Minnesota, USA), Dr. Edward Brooke and Isaac Westwood (University of Oxford, UK) for helpful discussions and advice. We are also grateful to the Wellcome Trust for financial support and the Oxford University Kobe foundation for a scholarship (A.K.). Syrian hamster liver samples were kindly donated by Olivia Hibbitt (University of Oxford, UK).

References

[1] Weber WW, Hein DW. Arylamine *N*-acetyltransferases. Pharmacol Rev 1985;37:25–79.
[2] Upton A, Johnson N, Sandy J, Sim E. Arylamine *N*-acetyltransferases of mice, men and microorganisms. Trends Pharmacol Sci 2001; 22(3):140–6.
[3] Payton M, Mushtaq A, Yu T-WW., Wu L-JJ., Sinclair J, Sim E. Eubacterial arylamine *N*-acetyltransferases – identification and comparison of 18 members of the protein family with conserved active site cysteine, histidine and aspartate residues. Microbiology 2001;147: 1137–47.
[4] Delomenie C, Fouix S, Longuemaux S, Brahimi N, Bizet C, Picard B, et al. Identification and functional characterization of arylamine *N*-acetyltransferases in eubacteria: evidence for highly selective acetylation of 5-aminosalicylic acid. J Bacteriol 2001;183(11):3417–27.
[5] Blum M, Grant DM, McBride W, Heim M, Meyer UA. Human arylamine *N*-acetyltransferase genes: isolation, chromosomal localization, and functional expression. DNA Cell Biol 1990;9(3):193–203.
[6] Ohsako S, Deguchi T. Cloning and expression of cDNAs for polymorphic and monomorphic arylamine *N*-acetyltransferases from human liver. J Biol Chem 1990;265(8):4630–4.
[7] Grant DM, Hughes NC, Janezic SA, Goodfellow GH, Chen HJ, Gaedigk A, et al. Human acetyltransferase polymorphisms. Mutat Res 1997;376:61–70.
[8] Hein DW. Molecular genetics and function of NAT1 and NAT2: role in aromatic amine metabolism and carcinogenesis. Mutat Res 2002;506–507:65–77.
[9] Hein DW, Doll MA, Fretland AJ, Leff MA, Webb SJ, Xiao GH, et al. Molecular genetics and epidemiology of the NAT1 and NAT2 acetylation polymorphisms. Cancer Epidemiol Biomarkers Prevention 2000;9(1):29–42.
[10] Grant DM, Blum M, Beer M, Meyer UA. Monomorphic and polymorphic human arylamine *N*-acetyltransferases: a comparison of liver isozymes and expressed products of two cloned genes. Mol Pharmacol 1991;39(2):184–91.
[11] Hickman D, Palamanda J, Unadkat J, Sim E. Enzyme kinetic properties of human recombinant arylamine *N*-acetyltransferase 2 allotypic variants expressed in *E. coli*. Biochem Pharmacol 1995; 50:697–703.
[12] Jenne JW. Partial purification and properties of the isoniazid transacetylase in human liver: its relationship to the acetylation of *p*-aminosalicylic acid. J Clin Invest 1965;44:1992–2002.
[13] Ilett KF, Ingram DM, Carpenter DS, Teitel CH, Lang NP, Kadlubar FF, et al. Expression of monomorphic and polymorphic *N*-acetyltransferases in human colon. Biochem Pharmacol 1994;47(5):914–7.
[14] Hickman D, Pope J, Patil SD, Fakis G, Smelt V, Stanley LA, et al. Expression of arylamine *N*-acetyltransferase in human intestine. Gut 1998;42(3):402–9.
[15] Cribb AE, Grant DM, Miller MA, Spielberg SP. Expression of monomorphic arylamine *N*-acetyltransferase (NAT1) in human leukocytes. J Pharmacol Exp Ther 1991;259(3):1241–6.
[16] Risch A, Smelt V, Lane D, Stanley L, van der Slot W, Ward A, et al. Arylamine *N*-acetyltransferase in erythrocytes of cystic fibrosis patients. Pharmacol Toxicol 1996;78(4):235–40.
[17] Stanley LA, Coroneos E, Cuff R, Hickman D, Ward A, Sim E. Immunochemical detection of arylamine *N*-acetyltransferase in normal and neoplastic bladder. J Histochem Cytochem 1996;44(9):1059–67.
[18] Smelt VA, Upton A, Adjaye J, Payton MA, Boukouvala S, Johnson N, et al. Expression of arylamine *N*-acetyltransferases in pre-term placentas and in human pre-implantation embryos. Hum Mol Genet 2000;9(7):1101–7.
[19] Ward A, Summers MJ, Sim E. Purification of recombinant human *N*-acetyltransferase type 1 (NAT1) expressed in *E. coli* and characterization of its potential role in folate metabolism. Biochem Pharmacol 1995;49(12):1759–67.
[20] Minchin RF. Acetylation of *para*-aminobenzoylglutamate, a folate catabolite, by recombinant human NAT and U937 cells. Biochem J 1995;307:1–3.
[21] Adam PJ, Berry J, Loader JA, Tyson KL, Craggs G, Smith P, et al. Arylamine *N*-acetyltransferase-1 is highly expressed in breast cancers and conveys enhanced growth and resistance to Etoposide in vitro. Mol Cancer Res 2003;1(11):826–35.
[22] Kadlubar FF, Minchin RF, Teitel CH, Turesky RJ, K.F I. ATP-dependent kinase-catalyzed activation of *N*-hydroxy hetero-cyclic amines. Drug Metab Rev 2002;34:53.
[23] Stanley LA, Copp AJ, Pope J, Rolls S, Smelt V, Perry VH, et al. Immunochemical detection of arylamine *N*-acetyltransferase during mouse embryonic development and in adult mouse brain. Teratology 1998;58(5):174–82.
[24] Cornish VA, Pinter K, Boukouvala S, Johnson N, Labrousse C, Payton M, et al. Generation and analysis of mice with a targeted disruption of the arylamine *N*-acetyltransferase type 2 gene. Pharmacogenomics J 2003;3(3):169–77.
[25] Sugamori KS, Wong S, Gaedigk A, Yu V, Abramovici H, Rozmahel R, et al. Generation and functional characterization of aryalmine *N*-acetyltransferase Nat1/Nat2 double-knockout mice. Mol Pharmacol 2003;64:170–9.
[26] Riddle B, Jencks WP. Acetyl-coenzyme A: arylamine *N*-acetyltransferase: role of the acetyl-enzyme intermediate and the effects of substituents on the rate. J Biol Chem 1971;246(10):3250–8.
[27] Sinclair JC, Sandy J, Delgoda R, Sim E, Noble ME. Structure of arylamine *N*-acetyltransferase reveals a catalytic triad. Nat Struct Biol 2000;7(7):560–4.
[28] Bhakta S, Besra GS, Upton AM, Parish T, Sholto-Douglas-Vernon C, Gibson KJ, et al. Arylamine *N*-acetyltransferase is required for synthesis of mycolic acids and complex lipids in *Mycobacterium bovis* BCG and represents a novel drug target. J Exp Med 2004; 199(9):1191–9.
[29] Floss H, Yu T-W. Lessons from the rifamycin biosynthetic gene cluster. Curr Opin Chem Biol 1999;3:592–7.
[30] Trinidad A, Kirlin WG, Ogolla F, Andrews AF, Yerokun T, Ferguson RJ, et al. Kinetic characterization of acetylator genotype-dependent and -independent *N*-acetyltransferase isozymes in homozygous rapid

and slow acetylator inbred hamster liver cytosol. Drug Metab Dispos 1989;17(3):238–47.

[31] Ozawa S, Abu-Zeid M, Kawakubo Y, Toyama S, Yamazoe Y, Kato R. Monomorphic and polymorphic isozymes of arylamine *N*-acetyltransferases in hamster liver: purification of the isozymes and genetic basis of *N*-acetylation polymorphism. Carcinogenesis 1990;11(12):2137–44.

[32] Abu-Zeid M, Nagata K, Miyata M, Ozawa S, Fukuhara M, Yamazoe Y, et al. An arylamine acetyltransferase (AT-I) from Syrian golden hamster liver: cloning, complete nucleotide sequence, and expression in mammalian cells. Mol Carcinog 1991;4(1):81–8.

[33] Nagata K, Ozawa S, Miyata M, Shimada M, Yamazoe Y, Kato R. Primary structure and molecular basis of polymorphic appearance of an acetyltransferase (AT-II)* in hamsters. Pharmacogenetics 1994;4(2):91–100.

[34] Ferguson RJ, Doll MA, Baumstark BR, Hein DW. Polymorphic arylamine *N*-acetyltransferase encoding gene (NAT2) from homozygous rapid and slow acetylator congenic Syrian hamsters. Gene 1994;140(2):247–9.

[35] Ferguson RJ, Doll MA, Rustan TD, Hein DW. Cloning, expression, and functional characterization of rapid and slow acetylator polymorphic *N*-acetyl-transferase encoding genes of the Syrian hamster. Pharmacogenetics 1996;6(1):55–66.

[36] Ferguson RJ, Doll MA, Rustan TD, Gray K, Hein DW. Cloning, expression, and functional characterization of two mutant (NAT2 (191) and NAT2 (341/803)) and wild-type human polymorphic *N*-acetyltransferase (NAT2) alleles. Drug Metab Dispos 1994; 22(3):371–6.

[37] Hein DW, Rustan TD, Martin WJ, Bucher KD, Miller LS, Furman EJ. Acetylator genotype-dependent N-acetylation of arylamines in vivo and in vitro by hepatic and extrahepatic organ cytosols of Syrian hamsters congenic at the polymorphic acetyltransferase locus. Arch Toxicol 1992;66(2):112–7.

[38] Sticha KR, Sieg CA, Bergstrom CP, Hanna PE, Wagner CR. Overexpression and large-scale purification of recombinant hamster polymorphic arylamine *N*-acetyltransferase as a dihydrofolate reductase fusion protein. Protein Expr Purif 1997;10(1):141–53.

[39] Hein DW, Doll MA, Fretland AJ, Gray K, Deitz AC, Feng Y, et al. Rodent models of the human acetylation polymorphism: comparisons of recombinant acetyltransferases. Mutat Res 1997;376(1–2):101–6.

[40] Wang H, Vath GM, Gleason KJ, Hanna PE, Wagner CR. Probing the mechanism of hamster arylamine *N*-acetyltransferase 2 acetylation by active site modification, site-directed mutagenesis, and pre-steady state and steady state kinetic studies. Biochemistry 2004;43(25):8234–46.

[41] Coroneos E, Gordon JW, Kelly SL, Wang PD, Sim E. Drug metabolising *N*-acetyltransferase activity in human cell lines. Biochim Biophys Acta 1991;1073(3):593–9.

[42] Ackers GK. Molecular exclusion and restricted diffusion processes in molecular-sieve chromatography. Biochemistry 1964;72:723–30.

[43] Wang H, Vath GM, Kawamura A, Bates CA, Sim E, Hanna PE, Wagner CR. Overexpression, purification and characterization of recombinant human arylamine *N*-acetyltransferase 1. Protein J, in press.

[44] Sandy J, Mushtaq A, Kawamura A, Sinclair J, Sim E, Noble M. The structure of arylamine *N*-acetyltransferase from *Mycobacterium smegmatis*—an enzyme which inactivates the anti-tubercular drug, isoniazid. J Mol Biol 2002;318(4):1071–83.

[45] Kawamura A, Sandy J, Upton A, Noble M, Sim E. Structural investigation of mutant *Mycobacterium smegmatis* arylamine *N*-acetyltransferase: a model for a naturally occurring functional polymorphism in *Mycobacterium tuberculosis* arylamine *N*-acetyltransferase. Protein Expr Purif 2003;27(1):75–84.

[46] Brooke EW, Davies SG, Mulvaney AM, Pompeo F, Sim E, Vickers RJ. An approach to identifying novel substrates of bacterial arylamine *N*-acetyltransferases. Bioorg Med Chem 2003;11(7):1227–34.

[47] Marti-Renom MA, Stuart AC, Fiser A, Sanchez R, Melo F, Sali A. Comparative protein structure modeling of genes and genomes. Annu Rev Biophys Biomol Struct 2000;29:291–325.

[48] Laskowski RA, MacArthur MW, Moss DS, Thornton JM. PROCHECK: a program to check the stereochemical quality of protein structures. J Appl Crystallogr 1993;26(2):283–91.

[49] McQueen CA, Weber WW. Characterization of human lymphocyte *N*-acetyltransferase and its relationship to the isoniazid acetylator polymorphism. Biochem Genet 1980;18(9–10):889–904.

[50] Sinclair J, Delgoda R, Noble M, Jarmin S, Goh N, Sim E. Purification, characterisation and crystallisation of an *N*-hydroxyarylamine *O*-acetyltransferase from *Salmonella typhimurium*. Prot Exp Purif 1998;12:371–80.

[51] Stanley LA, Mills IG, Sim E. Localization of polymorphic *N*-acetyltransferase (NAT2) in tissues of inbred mice. Pharmacogenetics 1997;7(2):121–30.

[52] Atmane N, Dairou J, Paul A, Dupret JM, Rodrigues-Lima F. Redox regulation of the human xenobiotic metabolizing enzyme arylamine *N*-acetyltransferase 1 (NAT1): reversible inactivation by hydrogen peroxide. J Biol Chem 2003;278(37):35086–92.

[53] Goodfellow GH, Dupret JM, Grant DM. Identification of amino acids imparting acceptor substrate selectivity to human arylamine acetyltransferases NAT1 and NAT2. Biochem J 2000;348(Part 1):159–66.

[54] Butcher NJ, Arulpragasam A, Minchin RF. Proteasomal degradation of *N*-acetyltransferase 1 is prevented by acetylation of the active site cysteine: a mechanism for the slow acetylator phenotype and substrate-dependent down-regulation. J Biol Chem 2004;279(21):22131–7.

[55] Butcher NJ, Ilett KF, Minchin RF. Substrate-dependent regulation of human arylamine *N*-acetyltransferase-1 in cultured cells. Mol Pharmacol 2000;57(3):468–73.

[56] Wakefield L, Cornish VA, Sim E. Expression of murine NAT2 during cardiac development. J Histochem Chytochem, in press.